Ultralow Emittance, Multi-MeV Proton Beams from a Laser Virtual-Cathode Plasma Accelerator

T. E. Cowan,[1,9] J. Fuchs,[1,2,9] H. Ruhl,[1,9] A. Kemp,[1,9] P. Audebert,[2] M. Roth,[3] R. Stephens,[1] I. Barton,[1] A. Blazevic,[3] E. Brambrink,[3] J. Cobble,[4] J. Fernández,[4] J.-C. Gauthier,[2] M. Geissel,[3] M. Hegelich,[4,5] J. Kaae,[1] S. Karsch,[5] G. P. Le Sage,[6] S. Letzring,[4] M. Manclossi,[7] S. Meyroneinc,[8] A. Newkirk,[1] H. Pépin,[2] and N. Renard-LeGalloudec[9]

[1]*General Atomics, San Diego, California 92121, USA*

[2]*Laboratoire pour l'Utilisation des Lasers Intenses, UMR 7605, CNRS-CEA-École Polytechnique-Université Paris VI, 91128 Palaiseau, France*

[3]*Gesellschaft für Schwerionenforschung, 64291 Darmstadt, Germany*

[4]*Los Alamos National Laboratory, University of California, Los Alamos, New Mexico 87545, USA*

[5]*Max-Planck-Institut für Quantenoptik, Garching, Germany*

[6]*Lawrence Livermore National Laboratory, University of California, Livermore, California 94550, USA*

[7]*Laboratoire d'Optique Appliquée, ENSTA-École Polytechnique, 91761 Palaiseau CEDEX, France*

[8]*Centre de Protonthérapie d'Orsay, 91402 Orsay, France*

[9]*Physics Department, MS-220, University of Nevada, Reno, Nevada 89557, USA*

(Received 9 November 2003; published 19 May 2004)

The laminarity of high-current multi-MeV proton beams produced by irradiating thin metallic foils with ultraintense lasers has been measured. For proton energies >10 MeV, the transverse and longitudinal emittance are, respectively, <0.004 mm mrad and $<10^{-4}$ eV s, i.e., at least 100-fold and may be as much as 10^4-fold better than conventional accelerator beams. The fast acceleration being electrostatic from an initially cold surface, only collisions with the accelerating fast electrons appear to limit the beam laminarity. The ion beam source size is measured to be <15 μm (FWHM) for proton energies >10 MeV.

DOI: 10.1103/PhysRevLett.92.204801 PACS numbers: 29.27.Fh, 52.38.Kd, 52.40.Kh, 52.70.Nc

The generation of high-current multi-MeV protons and ions by irradiating thin foils with short-pulse, ultrahigh intensity lasers ($\tau < ps$, $I\lambda^2 > 10^{18}$ W cm^{-2} μm^2) [1–5] is a promising new area of research and has renewed speculation for applications such as tabletop ion accelerators [6,7], high-resolution charged-particle radiography [8], or production of high energy density matter [9]. The interest in these ion beams lies in their potential high degree of laminarity and extremely low source size.

Our present understanding is that the high laminarity, or low emittance, of these beams stems from the fact the acceleration process takes place on the cold rear (i.e., nonirradiated) surface of the thin foils. There, a dense relativistic electron sheath is formed by the laser-accelerated electrons [1,3–5,10] that have propagated through the foil. This sheath produces an electrostatic field $>10^{12}$ V/m [11] that ionizes the surface atoms almost instantaneously, forming a $\sim$1 nm thick ion layer which, together with the electron sheath, resembles a virtual cathode (see Fig. 1). The resulting accelerated ion beam is composed mostly of protons originating primarily from contaminant layers of water vapor and hydrocarbons on the target surface [3,4]. As will be shown below, the extremely strong, transient acceleration that takes place from a cold, initially unperturbed surface, results in the low beam emittance that may be limited only by the collisions with the comoving electrons during the acceleration [12]. Such an acceleration process represents a new and potentially near-ideal kind of ion diode as compared either to the ion beams generated from plasma plumes [13], i.e., from the laser-heated turbulent plasma on the front side of the foils, or to the conventional plasma discharge ion sources used in accelerators.

Attempts have been made to measure the beam emittance or source size by using projection, on a far distant

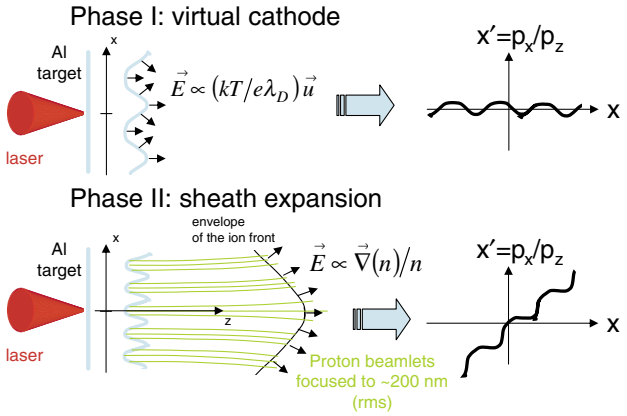

FIG. 1 (color online). Schematic of experiment. The laser pulse is focused on a foil having a modulated rear surface. Protons are first accelerated normal to the surface by the virtual cathode (VC) producing a modulation of the takeoff angle. The produced beamlets then expand with the quasineutral sheath. This adds an overall near-linear divergence to the beam initial angular modulation. Projected on a film stack far away, this results in a modulation of the dose, allowing one to image the VC stage magnified.

film, of objects such as knife edges [14] or meshes [15] placed in the ion beam path. The transverse emittance was estimated to be ≤ 0.5 mm mrad [14]. However, the ion beam does not propagate ballistically close to the target and passage of the beam on the object induces chargeup that deflects the beam. Therefore the beam emittance or source size cannot be reconstructed precisely from such measurements.

In this Letter, using a new technique that allows one to directly image the initial accelerating sheath and to fully reconstruct the transverse phase space, we experimentally show that, for protons of up to 10 MeV, the transverse emittance is as low as 0.004 mm mrad, i.e., 100-fold better than typical RF accelerators and at a substantially higher ion current (kA range). In addition, we show that the removal of the comoving electrons after 1 cm of beam expansion does not increase significantly the measured proton transverse emittance. This is the first demonstration of high-current laser-produced charged-particle beams with characteristics substantially superior to conventional accelerators. Also, we determine directly for the first time the size of the ion source, a crucial parameter for developments of high-resolution charged-particle radiography or ion patterned lithography.

The technique we developed for imaging the accelerating sheath uses target design that allows manipulating the ion beam generation during the initial, virtual-cathode phase of the acceleration by generating a stream of beamlets, within the expanding proton envelope, that can be used as fiducials of the acceleration.

The laminarity of charged-particle beams is characterized by their emittance [16], which is proportional to the volume of the bounding ellipsoid of the distribution of particles in phase space. By Liouville's theorem, the phase-space volume of a particle ensemble is conserved during nondissipative acceleration and focusing. For the transverse phase-space dimensions (here x-$p_x$for beam propagation along z), the area of the bounding phase-space ellipse equals $\pi\varepsilon_N$, where the root-mean-square (rms) value of the "normalized emittance" ε_N, at a specific beam energy (or momentum p), is expressed as $\varepsilon_N = (|\boldsymbol{p}|/mc)[\langle x^2\rangle\langle x'^2\rangle - \langle xx'\rangle^2]^{1/2}$, where m is the ion mass, c is the velocity of light, x is the particle position within the beam envelope, and $x' = p_x/p_z$ is the particles' divergence in the x direction. At a beam waist, $\varepsilon_N = \beta\gamma\sigma_x\sigma_{x'}$ where σ_x and $\sigma_{x'}$ are the rms values of the beamwidth and divergence angle. For typical proton accelerators [e.g., the CERN Super Proton Synchrotron (SPS)], the emittance from the proton injector linac is $\sim$1 mm mrad (normalized rms) and up to 3.5 mm mrad within the synchrotron, with 10^{11} protons per bunch. The longitudinal phase space (z-p_z) is characterized by the equivalent, energy-time product of the beam envelope and a typical value, for the CERN SPS, is $\sim$0.5 eV s. The highest quality ion beams have the lowest values of transverse and longitudinal emittance, indicating a low effective transverse ion temperature and a high degree of angle space and time-energy correlation.

We have assessed the characteristics of the laser-accelerated ion beams in experiments performed using the 100 TW short-pulse laser at the Laboratoire pour l'Utilisation des Lasers Intenses (LULI), and the 30 TW Trident laser at the Los Alamos National Laboratory. The concept of the experiment is shown schematically in Fig. 1. Laser pulses of $\sim$20–30 J of 1 μm light (350–850 fs) were focused onto the front surface of thin foils of Au or Al (10–50 μm thick). Note that the targets can be used only once since they are destroyed during the shot. The accelerated protons are detected in multiple layers of radiochromic film (RCF) densitometry media [17]. The spatial distribution of the protons in a given RCF layer gives the angular emission pattern at a specific interval of proton energy. By carefully preparing the rear surface of the target foil, and by shaping the laser focal intensity distribution, we controlled the virtual-cathode phase of the acceleration where the electric field is normal to the ion charge layer [10,18]. For the data of Figs. 2(a)–2(c), we used optically flat aluminum foils on the rear surface of which we micromachined shallow grooves, 200 nm deep spaced 3.6 μm apart. From a quantitative analysis of the film optical densities, we measure that $\sim 10^{11}$ protons are produced in a single laser shot for energies above 4 MeV, which corresponds to an ion current of >1 kA at 1 mm from the target foil. We observe a decrease in the angular envelope of the protons with increasing proton energy, as has been observed previously [3,4]. However, using the modulation of the beam intensity impressed during the initial phase, we are able to image the proton-emitting surface and thus to measure for the first time directly the source size. By accelerating protons off nonperiodic surface structures, as illustrated in Fig. 3, we

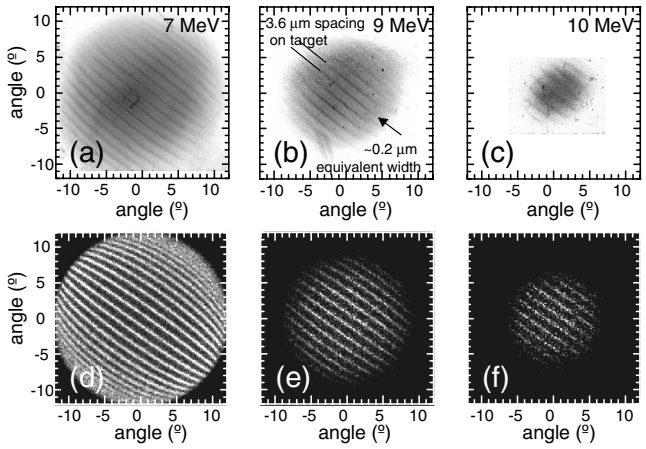

FIG. 2. (a)–(c) Angular distributions on RCF of protons accelerated from an 18 μm thick Al flat target irradiated at 10^{19} W/cm^2. (d)–(f) Simulated RCF images [same parameters and proton energies as in (a)–(c)] using a 3D PIC effective code.

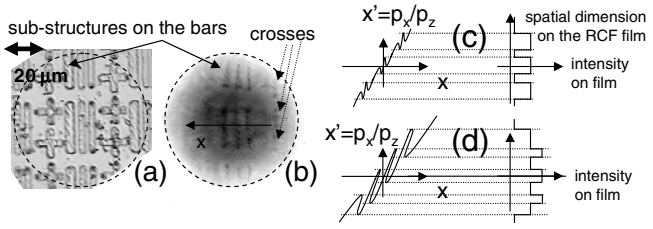

FIG. 3. (a) Image of a 48 μm thick Au target rear surface. (b) Resulting angular proton distribution at 8 MeV. The phase-space modulations induced by the surface structures produce corresponding intensity modulations, as illustrated in (c) for the case of the three parallel bars. Note that the modulations do not overlap; otherwise, as illustrated in (d), the proton dose between the bars would be different than the one outside, which is not the case.

verified that there is no overlap of the beam fiducials from adjacent structures that could lead to misinterpretation of the data. We establish that for protons above 4.5 MeV the decrease in the angular envelope with energy is due to a decrease of the emitting zone, but not due to a strong change in the divergence (i.e., magnification) of the beam envelope or from magnetic field deflection [2,19].

Such a decrease of the emission zone is expected for a transversally bell-shaped electron density distribution. In such a sheath, the highest energy protons are accelerated in the central, high-density portion of the sheath, whereas lower energies come from the wings of the sheath distribution and thus are emitted at a larger angle [18]. This comes from the accelerating field $E = -\nabla\Phi = -(kT_{\rm hot}/e)(\nabla n_{\rm hot}/n_{\rm hot})$, where $n_{\rm hot} \sim \exp[e\Phi(r)/kT_{\rm hot}]$ is the Boltzmann distribution of the hot electrons in the sheath. The measured diameter (FWHM) of the virtual-cathode emission zone is of the order of 70 μm at 4.5 MeV, 45 μm at 7 MeV, and $\sim$30 μm for $>$9 MeV protons.

In Fig. 4(a), we plot the divergence angle versus the source position of the accelerated protons by using the nanofocused structures as fiducial marks impressed in the initial beam. Note that within the central portion of the beam the phase-space correlation is almost exactly linear. This remarkable result suggests that the relativistic electron sheath has a nearly Gaussian-radial distribution in its density profile, which gives a nearly linear relation between radial position and the radial electric field in the sheath [18]. Note that this is supported by the 3D particle-in-cell (PIC) simulation which displays the same behavior as shown in Fig. 4(b).

By assuming that the protons in each beamlet come from an ideal line focus, we experimentally deduce an upper limit on the transverse emittance of $<$0.004 mm mrad for 10 MeV protons, a factor of $>$100 smaller than typical proton beam sources. We attribute this to the fact that during much of the acceleration the proton space charge is neutralized by the comoving hot electrons. PIC simulations show that the image generation is more complicated. Indeed, as shown in Fig. 4(b), the

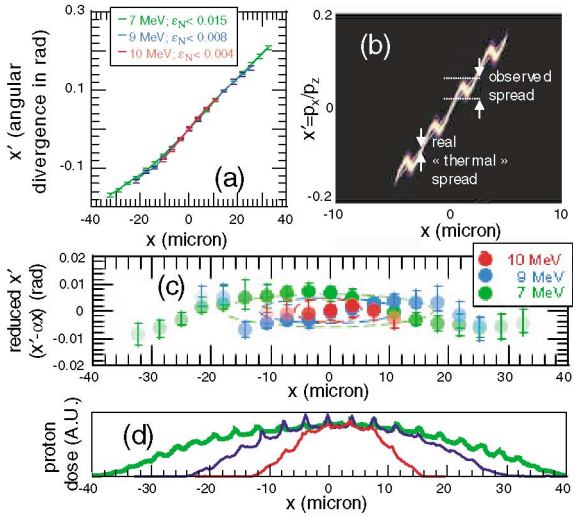

FIG. 4 (color). (a) Transverse phase space plot of the proton beam [from Figs. 2(a)–2(c)]. Error flags denote the rms angular width (1σ) of the beamlets. This gives an upper limit on envelope divergence, from which we estimate an upper limit of the emittance ε_N at each energy, as marked (in units mm mrad). (b) Same from the effective PIC simulation 600 fs after the interaction. (c) Same as (a) but in a rotated frame. The emittance ellipses using the Twiss parameters are overlaid. The transparencies of the dots encode the value of the dose at each point, following the curves shown in (d).

observed angular width of the beamlets, which is a projection in $x' = p_x/p_z$ of the transverse phase space, involves the magnitude of the initial transverse momentum oscillation (see Fig. 1) in addition to the irreducible thermal spread. Accordingly, the actual transverse emittance could be smaller than the deduced $<$0.004 mm mrad. The irreducible "thermal" contribution to the emittance can be interpreted as an effective proton transverse Maxwellian temperature ranging from $<$15 eV for the highest resolution portion of the data to $<$200 eV at the edge of the beam. The reconstructed RCF images in Figs. 2(d)–2(f) assumed a transverse proton temperature of 100 eV, which is consistent with the data but appears to overestimate the width of the highest resolution beamlets. Separate 1D PIC simulations that include binary collisions show a ratio of longitudinal to transverse ion temperature of $\sim 10^5$–10^6 for sheath-accelerated ions of $\sim$10 MeV [12]. Without collisions, the simulation does not exhibit any transverse ion temperature. This suggests that an ideal collisionless acceleration would produce a perfectly laminar beam but the collisional heating of the ions during the early virtual-cathode stage will set the absolute limit on the achievable emittance.

The energy spread of the laser-accelerated proton beam is large, ranging from 0–10 MeV; however, due to the extremely short duration of the accelerating field ($<$10 ps), the longitudinal phase-space energy-time product must be less than 10^{-4} eV s. The 3D PIC simulations show that longitudinally the acceleration is extremely

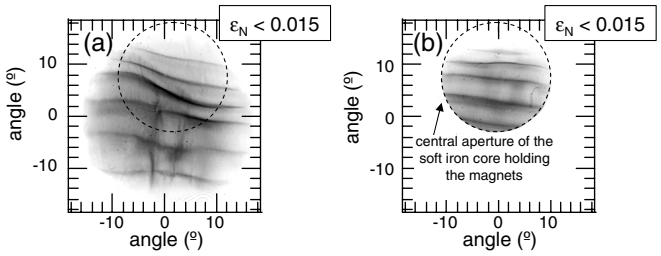

FIG. 5. Structured proton beam at ~6.5 MeV produced by a 10^{19} W/cm^2 pulse incident on a 40 μm thick Al foil. Observed ripples in the laser focal spot that can deform the bell-shaped sheath [18] are likely to induce the observed distortions in the beam. (a) Ion part of the neutralized beam detected; the RCF is placed 59 mm from the target (b) Non-neutral ion part of the beam.

laminar, in the sense that the spread of proton energies in a given longitudinal slice is very small. We estimate from the simulation an energy-time product of $<10^{-7}$ eV s. Such extremely good longitudinal velocity "chirp" of the beam is interesting since it could in principle allow one to monochromatize a portion of the beam by coupling it to the field gradient of a postaccelerator.

In order to take advantage of the exceptionally small proton beam emittance in future applications, e.g., to focus the ions or to capture them into a postaccelerator, removal of the comoving electrons without significantly perturbing the protons is crucial. As shown in Fig. 5, we tested if this could be done by comparing the situation where the neutralized plasma beam expands freely up to the RCF detector, or where we placed a 0.12 T pair of magnets 1 cm downstream from the target to remove all the electrons from the beam and let the non-neutral ion beam propagate 5 cm further to the RCF. A global increase of the ion beam envelope is expected for the non-neutral beam but no significant difference in the inferred emittance can be seen between the two shots. It shows that at this stage the removal, by the external B field, of the electrons that allowed the beam to accelerate laminarly does not increase the ion transverse temperature, such as might occur from turbulence in the electron trajectories resulting from the ion-induced space charge and the B field.

The potential impact of ultralow emittance, high-current laser-driven proton beams for accelerator physics could be significant. If the low transverse emittance could be maintained throughout the accelerator and up to the collision point of a high energy physics (HEP) machine, it would directly increase the luminosity and, hence, the discovery potential of existing facilities [20]. Such photohadron sources may impact the low energy booster section of HEP accelerators, by allowing smaller apertures and a higher bunch charge. Capture and postacceleration of such beams may also enable compact accelerators that could lead to a wider use of hadron beams for cancer therapy [21]. Finally, the beam laminarity is the enabling factor that could lead to significant progress in other applications, e.g., for radiography [8], generation of complex patterned beams, and for ion focusing to produce and/or probe high energy density matter and for fusion by fast ignition [9,22].

We acknowledge the expert support of the LULI and Trident laser teams, and useful discussions with G. Dugan. This work was supported by Grant No. E1127 from Région Ile-de-France, EU program HPRI CT 1999-0052, LANL Laboratory Directed Research & Development, corporate support of General Atomics, and UNR Grant No. DE-FC08-01NV14050.

[1] S. Hatchett *et al.*, Phys. Plasmas **7**, 2076 (2000).
[2] E. Clark *et al.*, Phys. Rev. Lett. **84**, 670 (2000).
[3] R. A. Snavely *et al.*, Phys. Rev. Lett. **85**, 2945 (2000).
[4] M. Roth *et al.*, Phys. Rev. ST Accel. Beams **5**, 061301 (2002).
[5] M. Hegelich *et al.*, Phys. Rev. Lett. **89**, 085002 (2002).
[6] D. Habs *et al.*, Prog. Part. Nucl. Phys. **46**, 375 (2001).
[7] I. Spencer *et al.*, Nucl. Instrum. Methods Phys. Res., Sect. B **183**, 449 (2001).
[8] M. Borghesi *et al.*, Plasma Phys. Controlled Fusion **43**, A267 (2001); J. A. Cobble *et al.*, J. Appl. Phys. **92**, 1775 (2002).
[9] P. Patel *et al.*, Phys. Rev. Lett. **91**, 125004 (2003).
[10] H. Ruhl *et al.*, Phys. Plasmas **11**, L17 (2004).
[11] S. Wilks *et al.*, Phys. Plasmas **8**, 542 (2001).
[12] A. Kemp *et al.* (to be published).
[13] S. J. Gitomer *et al.*, Phys. Fluids **29**, 2679 (1986).
[14] T. E. Cowan *et al.*, in *High Brightness Beams* (World Scientific, Singapore, 2000).
[15] M. Borghesi *et al.*, Phys. Rev. Lett. **92**, 055003 (2004).
[16] S. Humphries, *Charged Particle Beams* (Wiley, New Jersey, 1990).
[17] N. V. Klassen *et al.*, Med. Phys. **24**, 1924 (1997).
[18] J. Fuchs *et al.*, Phys. Rev. Lett. **91**, 255002 (2003).
[19] Y. Murakami *et al.*, Phys. Plasmas **8**, 4138 (2001).
[20] W. Chou, in *Proceedings of the 1999 Particle Accelerator Conference*, edited by A. Luccio and W. MacKay (IEEE, New York, 1999), p. 3285.
[21] A. L. Boyer *et al.*, Phys. Today **55**, No. 9, 34 (2002).
[22] M. Roth *et al.*, Phys. Rev. Lett. **86**, 436 (2001).